Surface polaron formation in the Holstein model

Reza Nourafkan
Department of Physics, Sharif University of Technology, P.O. Box 11155-9161, Tehran, Iran

Massimo Capone
SMC, CNR-INFM and Dipartimento di Fisica, Università Sapienza, P.le Aldo Moro 2, I-00185 Roma, Italy

Nasser Nafari
Institute for Research in Fundamental Sciences (IPM), P.O. Box 19395-5531, Tehran, Iran

(Received 11 May 2009; revised manuscript received 2 October 2009; published 23 October 2009)

The effect of a solid-vacuum interface on the properties of a strongly coupled electron-phonon system is analyzed using dynamical mean-field theory to solve the Holstein model in a semi-infinite cubic lattice. Polaron formation is found to occur more easily, i.e., for a weaker electron-phonon coupling, on the surface than in the bulk. On the other hand, the metal-insulator transition associated with the binding of polarons takes place at a unique critical strength in the bulk and at the surface.

DOI: 10.1103/PhysRevB.80.155130 PACS number(s): 71.30.+h, 73.20.−r, 71.38.Ht

I. INTRODUCTION

Convincing experimental evidence of polaronic behavior has been reported in materials such as the high-T_c cuprates and manganites. For instance, the transition from the low-temperature ferromagnetic metallic state to the paramagnetic insulating state in manganites is caused by the formation of combined structural/magnetic polarons.[1] Signatures of small polarons have been observed in undoped cuprates.[2,3]

From a theoretical point of view, polaron formation has been intensively studied using a number of approaches.[4–15] The dynamical mean-field theory (DMFT) (Ref. 16) as a powerful nonperturbative tool has proved to be an important method for improving our understanding of polaronic phenomena occurring in strongly correlated electron systems. DMFT is a powerful nonperturbative tool for strongly interacting systems. This technique, which becomes exact in the limit of infinite coordination number, reduces the full lattice many-body problem to a local impurity embedded in a self-consistent effective bath of free electrons.

DMFT studies of the half-filled Holstein model in a Bethe lattice with a semielliptic free density of states have clarified the difference between the polaron crossover, i.e., the continuous and progressive entanglement between electrons and phonons, and the bipolaronic metal-insulator transition.[17–19] If no symmetry breaking is allowed, for small electron-phonon (e-ph) couplings the ground state is metallic with Fermi-liquid characteristic. Upon increasing the e-ph coupling, the carriers lose mobility, eventually acquiring polaronic character, with a finite lattice distortion associated with the electron motion. Polaron formation occurs as a continuous crossover. Once formed, polarons tend to attract and form a bound pair in real space, called bipolaron.[17] Within DMFT the bipolaronic binding gives rise to an insulating state of localized pairs[20] and bipolaron formation gives rise to a metal-insulator transition. The pairing transition does not coincide with the polaron crossover: Polarons are formed before, i.e., for a weaker coupling, the pairing transition occurs as long as the typical phonon frequency is smaller than the electronic energy scales (adiabatic regime).

On the other hand, fabrication of a variety of heterostructures and interfaces involving cuprates and manganites raises the question of whether the electronic behavior at the surface or interface is different from the bulk. Several studies using DMFT have been devoted to the case of repulsive electron-electron interactions (Hubbard model) and to a vacuum-solid interface.[21] Potthoff and Nolting,[24] and Liebsch[25] have argued that reduced coordination at the surface may enhance correlation effects. They also studied the magnetic ordering induced by enhanced correlation at the surface. Matzdorf *et al.*[26] proposed that ferromagnetic ordering is stabilized at the surface by a lattice distortion. Surface ferromagnetism had been also discussed in a dynamical mean-field theory of Hubbard model by Potthoff and Nolting.[27] Helmes *et al.*[28] studied the scaling behavior of the metallic penetration depth into the Mott insulator near the critical Coulomb interaction within the Hubbard model. Borghi *et al.*[29] have shown the existence of a dead surface layer with exponentially suppressed quasiparticles.

Here we concentrate on the effect of a vacuum-solid surface on interacting electron-phonon systems, and study the formation of polarons and the transition to a bipolaronic insulating state in the semi-infinite Holstein model at half filling and zero temperature. The lattice is assumed to be a bipartite simple cubic (sc) with nearest-neighbor hopping. While the occurrence of charge transfer is typical for a system with reduced translational symmetry, in our model at half filling any charge transfer is excluded by the particle-hole symmetry, leading to a homogeneous charge distribution among the layers parallel to the surface, and local occupations near the surface do not differ from the average filling, $\langle n_\alpha \rangle = \langle n \rangle = 1$, where α labels each layer.

In addition to the geometrical effect of missing neighbors, the surface electronic structure of interacting electron systems is also complicated by the fact that the microscopic interactions in the vicinity of the surface have values which may significantly differ from those in the bulk. A relaxation of the surface layer, for example, changes the overlap between the one-particle basis states and thus implies a modified hopping integral. Within the Holstein model, the param-

eter modifications will be reflected in different values of the surface topmost layer hopping integrals and e-ph coupling strengths relative to the bulk ones. In this work we will not consider this effect, in order to focus on the more intrinsic effects that can give rise to different physics in the surface.

This paper is organized as follows: in Sec. II the model is introduced and the application of DMFT for surface geometry is briefly discussed. We mainly characterized the electronic and phononic properties by considering the layer quasiparticle weights, double occupancies, and the phonon probability-distribution function (PDF). The corresponding results are discussed in Sec. III. Finally Sec. IV is devoted to concluding remarks.

II. MODEL AND METHOD

The Holstein Hamiltonian is defined by

$$H = -t\sum_{\langle ij\rangle\sigma}(c_{i\sigma}^{\dagger}c_{j\sigma} + \text{c.c.}) + g\sum_{i}(n_i - 1)(b_i^{\dagger} + b_i) + \Omega_0\sum_{i} b_i^{\dagger}b_i, \tag{1}$$

where $c_{i\sigma}(c_{i\sigma}^{\dagger})$ and $b_i(b_i^{\dagger})$ are, respectively, destruction (creation) operators for itinerant electrons with spin σ and local vibrons of frequency $\Omega_0=0.2t$ on site i, n_i is the electron density on site i, t stands for the itinerant electrons hopping-matrix elements between the nearest-neighbor sites, and g denotes the electron-phonon coupling. We fix the energy scale by setting $t=1$.

To obtain the ground-state properties of this model, we use the embedding approach introduced by Ishida and Liebsch[30] to extend DMFT to inhomogeneous systems. In this scheme, the system is divided into two parts: the surface region which includes the first N layers and the adjacent semi-infinite bulk region (substrate) which is coupled to it. Next, we represent the effects of the substrate on the surface region by a complex, energy-dependent, embedding potential acting on the Hamiltonian matrix of the surface region. The embedding method requires to consider a relatively small number of surface layers and it is therefore a computationally less expensive extension of DMFT in the presence of an interface as compared to the slab method, in which the inhomogeneous system is simply represented as a finite number of layers.[30]

Because of translational symmetry in the plane parallel to the interface, the embedding potential of the substrate is diagonal with respect to the two-dimensional wave vector $\mathbf{k}=(k_x,k_y)$ and can be expressed as an $N\times N$ matrix by

$$\mathbf{S}(\mathbf{k},i\omega_n) = \tilde{\mathbf{T}}\mathbf{G}(\mathbf{k},i\omega_n)\mathbf{T}, \tag{2}$$

where $\mathbf{G}(\mathbf{k},i\omega_n)$ is the Green's function of the substrate defined by

$$\mathbf{G}(\mathbf{k},i\omega_n) = [(i\omega_n+\mu)\mathbf{1} - \boldsymbol{\epsilon}(\mathbf{k}) - \boldsymbol{\Sigma}(i\omega_n)]^{-1}. \tag{3}$$

In here, $\boldsymbol{\Sigma}(i\omega_n)$ is the bulk self-energy, which in the framework of single-site DMFT, is independent of wave vectors, $\mathbf{k}$, and ω_n are the Matsubara frequencies. We obtain the self-energy by performing a standard DMFT calculation for the bulk crystal corresponding to the substrate. μ is the chemical potential and $\boldsymbol{\epsilon}(\mathbf{k})$ is the two-dimensional dispersion relation, which includes information about surface geometry. The $\boldsymbol{\epsilon}(\mathbf{k})$ matrix for the surface cutting a simple cubic lattice along the z direction [sc(001) surface] takes the following form:[24]

$$\boldsymbol{\epsilon}(\mathbf{k}) = \begin{pmatrix} t\epsilon_{\parallel}(\mathbf{k}) & t\epsilon_{\perp}(\mathbf{k}) & 0 & 0 \\ t\epsilon_{\perp}(\mathbf{k}) & t\epsilon_{\parallel}(\mathbf{k}) & t\epsilon_{\perp}(\mathbf{k}) & 0 \\ 0 & t\epsilon_{\perp}(\mathbf{k}) & t\epsilon_{\parallel}(\mathbf{k}) & \cdots \\ 0 & 0 & \cdots & \cdots \end{pmatrix}. \tag{4}$$

The intralayer (parallel) hopping and the interlayer (perpendicular) hopping are specified by $t\epsilon_{\parallel}(\mathbf{k})$ and $t\epsilon_{\perp}(\mathbf{k})$, respectively, and are given by

$$\epsilon_{\parallel} = -2[\cos(k_x) + \cos(k_y)], \quad |\epsilon_{\perp}(\mathbf{k})|^2 = 1. \tag{5}$$

Finally, $\mathbf{T}$ is the hopping matrix between primitive cells of substrate and surface region. Since $\mathbf{T}$ is nonzero between nearest-neighbor layers of substrate and surface region, only the surface Green's function[31] of the substrate need to be considered in Eq. (2).

After constructing the embedding potential of the substrate, $\mathbf{S}(\mathbf{k},i\omega_n)$, by way of a coupled-layer DMFT calculation in the surface region the self-energy matrix is determined self-consistently. This can be achieved via the following steps: (i) associating an effective impurity model with each layer in the surface region, solving them by using an impurity solver to find the layer-dependent local self-energies, $\Sigma_{\alpha}(i\omega_n)$, and constructing the surface-region self-energy matrix which is diagonal in layer indices (α,β) with the elements, $\Sigma_{\alpha\beta}(i\omega_n)=\Sigma_{\alpha}(i\omega_n)\delta_{\alpha\beta}$, (ii) calculating the on-site layer-dependent Green's function via the following relation:

$$G_{\alpha}(i\omega_n) = \sum_{\mathbf{k}}\left(\frac{1}{(i\omega_n+\mu)\mathbf{1} - \boldsymbol{\epsilon}(\mathbf{k}) - \mathbf{S}(\mathbf{k},i\omega_n) - \boldsymbol{\Sigma}(i\omega_n)}\right)_{\alpha\alpha}, \tag{6}$$

where $N\times N$ $\boldsymbol{\epsilon}(\mathbf{k})$ matrix is given by Eq. (4), and (iii) implementing the DMFT self-consistency relation for each layer, $\mathcal{G}_{\alpha}^{0}(i\omega_n)=[G_{\alpha}^{-1}(i\omega_n)+\Sigma_{\alpha}(i\omega_n)]^{-1}$, which determines the bath parameters for the new effective impurity model. The cycles have to be repeated until self-consistency is achieved.

We use the exact diagonalization (ED) technique to solve the effective impurity model at zero temperature.[32] The ED technique works equally well for any values of the parameters and only involves a discretization of the bath hybridization function, which is described in terms of a finite and small set of levels n_s for the purpose of limiting the Hilbert space to a workable size. For the case of phonon degrees of freedom we considered here, the infinite phonon space is also truncated allowing for a maximum number of excited phonons N_{ph}. The typical values we considered for the bath levels are $n_s=8-9$ and typical maximum number of phonons are $N_{ph}=30-50$. We tested that these numbers, indeed, provide converged results. Moreover, for the reasons discussed in Sec. III the number of surface layers is chosen to be $N=5$ throughout our calculations.

III. RESULTS

As mentioned in Sec. I, all our calculations are performed for the case of uniform parameters. This assumption, together with the half-filling condition which enforces charge homogeneity, allows us to single out the effect of the interface and to focus on the purely geometrical aspect of the problem. Even in the absence of any surface reconstruction, the reduced coordination of atoms causes a characteristic oscillatory variation in the free local density of states (LDOS) as a function of layer index, with a significant narrowing of the surface LDOS as compared with the bulk.[31] The band narrowing can be understood by referring to the moments of the LDOS, $\rho_i^{(0)}(E)$. The moments are defined as[33]

$$M_i^{(m,0)} = \int_{-\infty}^{\infty} E^m \rho_i^{(0)}(E) dE = \sum_{i_1 \ldots i_{m-1}} t_{ii_1} t_{i_1 i_2} \ldots t_{i_{m-1} i}, \quad (7)$$

where i_m's refer to the sites of the semi-infinite lattice and t_{ij} is the hopping amplitude between site i and j, which is assumed to be nonzero only for nearest-neighbor sites and to be constant throughout the system, i.e., $t_{ij}=t$ for nearest neighbors. Using Eq. (7) the second moment is given by

$$\Delta^2 \rho_i^{(0)} = M_i^{(2,0)} - (M_i^{(1,0)})^2 = \sum_{j \neq i} t_{ij}^2 = q_i t^2, \quad (8)$$

where q_i is the coordination number of site i. For the surface of the sc lattice with normal along (001) direction, the coordination number for a site in the surface layer is $q_i=5$ while the bulk coordination number is $q_i=6$. The reduced coordination number of a site in the surface layer thus implies a reduced variance $\Delta^2\rho^{(0)}$ of the surface LDOS. Thus the delocalizing effect of the kinetic energy is weaker at the surface, and even if the electron-phonon coupling is identical at the surface and in the bulk, it will be more effective at the surface, which will show stronger-coupling physics. The same physics would act in the case of a solid-solid interface, in which the interface would be characterized by a different (smaller) hopping t', or in the case of defects also reducing some hopping-matrix elements.

In the case of an interface, the second and all subsequent layers have the same second moment of the bulk. However, despite the band-narrowing effect discussed above, the densities of states of all layers have the same band edges and their width is given by the width of the free bulk DOS.[33]

Figure 1 shows the calculated quasiparticle weight z_α of the semi-infinite Holstein model at $T=0$ in the metallic range as a function of layer index α, where the outermost layer corresponds to $\alpha=1$. z_α measures the metallic nature of a system, $z=1$ is for a noninteracting metal, and $z=0$ is for a correlated insulator. In our case $z=0$ implies a bipolaronic insulator. The crosses on the vertical axis on the right-hand side show the z values of the bulk metal determined by a separate bulk DMFT calculation. For any value of the coupling, the quasiparticle weight of the surface layer $z_{\alpha=1}$ is significantly reduced compared to $z_{\alpha=2}$ and $z_{\alpha=3}$ which can be understood as the effect of the reduced surface coordination number and enhanced effective correlations, in complete analogy to the results for repulsive interactions. The evolution as a function of the layer index depends instead on the

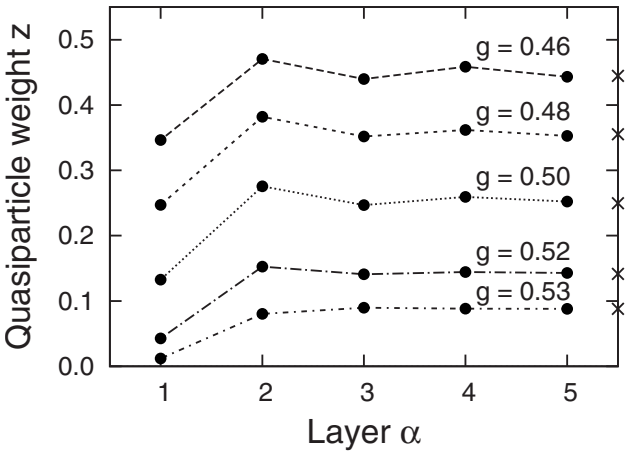

FIG. 1. Quasiparticle weight z of semi-infinite Holstein model for simple cubic lattice in the (001) orientation as a function of layer index α. Crosses on the vertical axis on the right-hand side indicate the bulk z corresponding to five given values of g. Lines are drawn as a guide to the eyes.

coupling regime. For weak and moderate e-ph couplings, z_α has a nonmonotonic behavior which is damped with increasing distance to the surface. For g values closer to the critical coupling strength of the bulk bipolaronic transition, g_c($g_c \approx 0.55$) the behavior changes qualitatively. Here the layer dependence becomes monotonic and the quasiparticle weight quickly approaches its bulk value with increasing α.

Top panel of Fig. 2 illustrates the layer-dependent quasiparticle weight z_α for the first three layers and the bulk quasiparticle weight as a function of g. As expected, all the z's monotonically decrease as a function of the e-ph coupling and they eventually vanish. As can be seen in the figure, the differences between the z_α and the bulk z diminish with increasing distance from the surface and for the third layer, the quasiparticle weight is almost indistinguishable from the bulk z on the scale used. It is crucial to observe that the different z_α all vanish at *the same* value of g, which also coincides with the bulk critical coupling strength, $g_c=g_{c,bulk}$.

If the surface and the bulk were decoupled, the reduced surface coordination number would tend to drive the surface to an insulating phase at a coupling strength lower than the bulk critical coupling g_c. However, below g_c the bulk excitations, due to hopping processes between the surface and the bulk can induce a quasiparticle peak with a nonzero weight $z_{\alpha=1}>0$ in the topmost layer and a real surface transition is not found, i.e., $z_{\alpha=1}$ remain nonzero, although being very small, up to the critical coupling for bulk transition, g_c. The investigation of the imaginary part of the layer-dependent self-energies, $\Sigma_\alpha(i\omega_n)$ at $\omega_n \to 0$ (middle panel of Fig. 2) confirms the uniqueness of the critical strength g_c. In the limit of $\omega_n \to 0$ and for all $g<g_c$, the imaginary part of self-energy vanishes for all layers as it is the case of a Fermi liquid. In the coupling constants close to g_c and in the metallic regime, a significant layer dependence of Im $\Sigma_\alpha(i\omega_n)$ for $\omega_n \to 0$ with a considerably larger slope in the first layer ($\alpha=1$) is seen, which reflects the enhanced correlation effects at the surface. In the insulating state, Im $\Sigma_\alpha(i\omega_n)$ diverges for $\omega_n \to 0$. Therefore, there is a unique critical

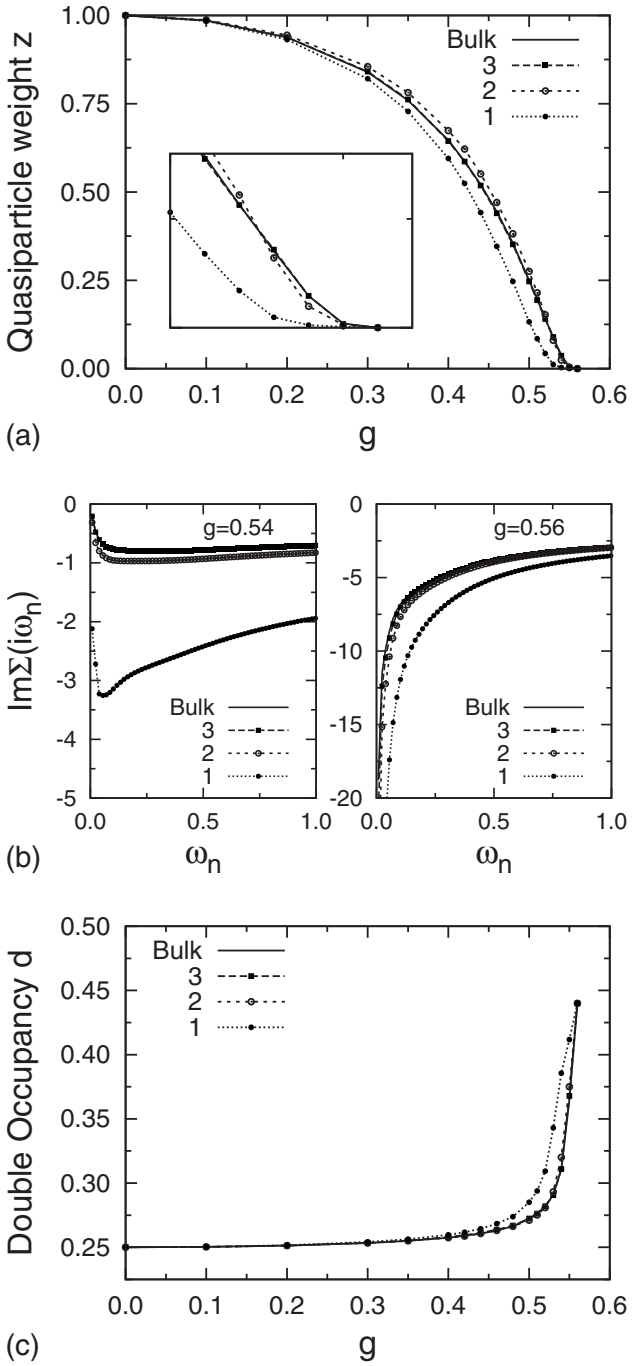

FIG. 2. Top panel: Layer-dependent quasiparticle weight z_α for the first three layers of the semi-infinite Holstein model with simple cubic (001) surface geometry and the bulk quasiparticle weight as a function of e-ph coupling strength, g. $\alpha=1$ stands for the topmost surface layer. The solid line shows z for bulk calculations. The inset shows $z_\alpha(g)$ in the critical regime. Middle panel: Imaginary part of the layer-dependent self-energy Σ_α on the discrete mesh of the imaginary energies $i\omega_n=(2n+1)\pi/\tilde{\beta}(\tilde{\beta}=400)$. Bottom panel: Layer-dependent double occupancy d_α as a function of g.

strength g_c at which all quasiparticle weight functions, $z_\alpha(g)$, simultaneously approach zero.

The layer-dependent average double occupancy, $d_\alpha=\langle n_{\alpha\uparrow}n_{\alpha\downarrow}\rangle$, is shown in the bottom panel of Fig. 2 as a function of g. For small g and all layers, d_α increases gradually.

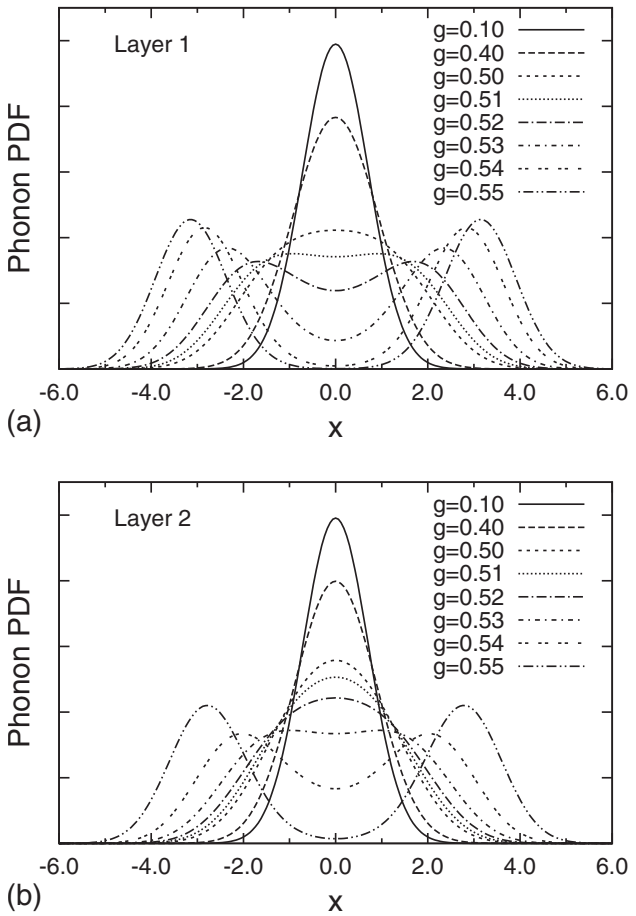

FIG. 3. Phonon probability-distribution function for the first and second surface layers of a semi-infinite sc(001) Holstein model at half filling. The various curves refer to different values of electron-phonon coupling strength, g. Upon increasing the e-ph coupling, a smooth crossover occurs between a unimodal distribution and a bimodal distribution. However, the polaron crossover (onset of bimodality) occurs at different values of g for the first and second layers. Top panel shows that at the topmost surface layer, polaron formation takes place at $g_{pol,1}\approx 0.51$ whereas at the second layer, it takes place at $g_{pol,bulk}\approx 0.53$ (bottom panel). All other layers behave just like the second layer.

At $g=g_c$ it rapidly reaches $\approx 1/2$. In the metallic region, the double occupancies are increased more rapidly at the topmost surface layer as compared with the interior of the system. Again, this is due to the stronger effective e-ph interaction which results from the narrowing of the noninteracting density of states at the surface.

We have thus far established that even in the presence of a surface, the half-filled Holstein model undergoes a single bipolaronic metal-insulator transition, despite the surface is less metallic than the bulk for any $g<g_c$. We now discuss how the surface influences the local lattice distortions, measured by the phonon PDF, $P(x)=\langle\phi_0|x\rangle\langle x|\phi_0\rangle$, where $|x\rangle\langle x|$ is the projection operator on the subspace for which the phonon displacement $\hat{x}$ has a given value x, and $|\phi_0\rangle$ is the ground-state vector. This quantity can be used to characterize the polaron crossover.[34]

In the absence of e-ph interaction $P(x)$ is a Gaussian centered around $x=0$. A small e-ph coupling slightly broadens

the distribution which remains centered around $x=0$, implying that the coupling is not sufficient to give rise to a finite polarization of the lattice. Continuously increasing the interaction one eventually obtains a bimodal distribution with two identical maxima at $x=\pm x_0$. Those maxima are indeed associated with empty and doubly occupied sites, and testify the entanglement between the electronic state and the lattice distortion, which is precisely the essence of the polaron crossover. Thus, the appearance of a bimodal shape in $P(x)$ is a marker of the polaron crossover.[18,34]

Figure 3 shows the polaron crossover for our semi-infinite Holstein model. For each layer the evolution as a function of the coupling follows the pattern we described above. The anharmonicity due to e-ph interaction increases with increasing coupling strength leading first to a non-Gaussian and finally to a bimodal PDF at all $g > g_{pol}$. This behavior signals the appearance of static distortions, even if we are neglecting any ordering between them. The strongest differences with respect to the bulk PDF are found for the top layer ($\alpha=1$) PDF. The layer PDFs converge to the bulk PDF with increasing distance to the surface. Beyond the third layer the PDF is essentially identical to its bulk behavior. Moreover, for the second layer, the shape of peaks could be slightly different but the position of the bimodality is the same as for the bulk. It is apparent from the data of Fig. 3 that the PDF at the topmost (surface) layer becomes bimodal at lower values of the coupling strength with respect to the internal layers. At the topmost surface layer, polaron formation takes place at $g_{pol,1} \approx 0.51$ whereas at the second layer and all the subsequent layers, it takes place at $g_{pol,bulk} \approx 0.53$. the surface can display polaronic distortions while the bulk is still undistorted (even if the local vibrations are strongly anharmonic).

IV. CONCLUDING REMARKS

We have investigated polaron formation and transition to the bipolaronic insulating state at solid-vacuum surface at zero temperature in the framework of the semi-infinite Holstein model at half filling. Using the embedding approach to extend dynamical mean-field theory to layered systems, it is found that the bipolaronic insulating state occurs simultaneously at the surface and in the bulk, and it takes place exactly at the same critical coupling strength found for the infinitely extended system, $g_{c,bulk}=g_c$. When the system is metallic the topmost layer quasiparticle weight z_1 is smaller than the bulk value z_{bulk} since a reduced surface coordination number implies a stronger effective correlation effects. Fixing the coupling at values quite smaller than g_c, the quasiparticle weight is an oscillating function of the layer index. As the distance from the surface increases, these oscillations fade away. For couplings close to the metal-insulator transition z_α instead increases monotonically by approaching the bulk. On the other hand, the polaron crossover occurs more easily at the surface with respect to the bulk. There is therefore a finite window of e-ph coupling in which the surface presents polaronic distortions while the bulk has no distortions. As we already mentioned, this difference is not able to support a metallic bulk coexisting with an insulating surface. We test our results for larger phonon frequencies, for example, $\Omega_0=2.0t$, and find that the general trend of these results hold in the antiadiabatic cases as well.

Surface effects are expected to be more pronounced as the number of missing neighbors in the topmost layer becomes larger. As we move from the sc(001) to the sc(011) and to the sc(111) surface geometries, the surface coordination numbers decrease from $n_c^{(001)}=5$ to $n_c^{(011)}=4$ to $n_c^{(111)}=3$, respectively. Therefore, we expect to observe a narrowed topmost layer free density of states which results in an enhanced ratio between the e-ph coupling strength and the effective bandwidth. Consequently, the e-ph interaction tends to be stronger at the surface. Clearly, according to this argument we expect the difference between the two coupling strengths for the polaron formation at the surface and in the bulk would become larger.

The present study has been restricted to uniform model parameters. This leaves several open questions such as the possibility of coexisting different surface and bulk phases, if the model parameters at the vicinity of the surface are modified. Indeed nonuniform parameters may lead to a a different physics in a repulsive Hubbard model.[29]

ACKNOWLEDGMENTS

M.C. acknowledges financial support of MIUR PRIN 2007 under Prot. No. 2007FW3MJX003.

[1] J. W. Lynn, D. N. Argyriou, Y. Ren, Y. Chen, Y. M. Mukovskii, and D. A. Shulyatev, Phys. Rev. B **76**, 014437 (2007).
[2] P. Calvani, M. Capizzi, S. Lupi, P. Maselli, A. Paolone, and P. Roy, Phys. Rev. B **53**, 2756 (1996).
[3] K. M. Shen, F. Ronning, D. H. Lu, W. S. Lee, N. J. C. Ingle, W. Meevasana, F. Baumberger, A. Damascelli, N. P. Armitage, L. L. Miller, Y. Kohsaka, M. Azuma, M. Takano, H. Takagi, and Z.-X. Shen, Phys. Rev. Lett. **93**, 267002 (2004).
[4] H. De Raedt and A. Lagendijk, Phys. Rev. B **27**, 6097 (1983).
[5] F. Marsiglio, Phys. Rev. B **42**, 2416 (1990).
[6] V. V. Kabanov and O. Yu. Mashtakov, Phys. Rev. B **47**, 6060 (1993).
[7] F. Marsiglio, Physica C **244**, 21 (1995); E. V. L. de Mello and J. Ranninger, Phys. Rev. B **55**, 14872 (1997).
[8] G. Wellein and H. Fehske, Phys. Rev. B **56**, 4513 (1997); H. Fehske and S. A. Trugman, in *Polarons in Advanced Materials* Springer Series in Material Sciences Vol. 103, edited by A. S. Alexandrov (Springer-Verlag, Dordrecht 2007), pp. 393–461.
[9] M. Capone, W. Stephan, and M. Grilli, Phys. Rev. B **56**, 4484 (1997); S. Ciuchi, F. de Pasquale, S. Fratini, and D. Feinberg, *ibid.* **56**, 4494 (1997); M. Capone, S. Ciuchi, and C. Grimaldi, Europhys. Lett. **42**, 523 (1998); M. Capone, M. Grilli, and W. Stephan, Eur. Phys. J. B **11**, 551 (1999).
[10] E. Jeckelmann and S. R. White, Phys. Rev. B **57**, 6376 (1998).

[11] V. Cataudella, G. De Filippis, and G. Iadonisi, Phys. Rev. B **62**, 1496 (2000).
[12] G. Kalosakas, S. Aubry, and G. P. Tsironis, Phys. Rev. B **58**, 3094 (1998).
[13] Li-Chung Ku, S. A. Trugman, and J. Bonca, Phys. Rev. B **65**, 174306 (2002).
[14] A. Macridin, B. Moritz, M. Jarrell, and T. Maier, Phys. Rev. Lett. **97**, 056402 (2006).
[15] G. L. Goodvin, M. Berciu, and G. A. Sawatzky, Phys. Rev. B **74**, 245104 (2006).
[16] A. Georges, G. Kotlier, W. Krauth, and M. J. Rozenberg, Rev. Mod. Phys. **68**, 13 (1996).
[17] M. Capone and S. Ciuchi, Phys. Rev. Lett. **91**, 186405 (2003).
[18] M. Capone, P. Carta, and S. Ciuchi, Phys. Rev. B **74**, 045106 (2006).
[19] D. Meyer, A. C. Hewson, and R. Bulla, Phys. Rev. Lett. **89**, 196401 (2002); J. K. Freericks, M. Jarrell, and D. J. Scalapino, Phys. Rev. B **48**, 6302 (1993); J. K. Freericks, *ibid.* **48**, 3881 (1993); A. J. Millis, R. Mueller, and B. I. Shraiman, *ibid.* **54**, 5389 (1996); P. Benedetti and R. Zeyher, *ibid.* **58**, 14320 (1998).
[20] M. Keller, W. Metzner, and U. Schollwöck, Phys. Rev. Lett. **86**, 4612 (2001); M. Capone, C. Castellani, and M. Grilli, *ibid.* **88**, 126403 (2002).
[21] The accuracy of DMFT for three-dimensional systems has been repeatedly shown. Indeed, combining DMFT with density-functional theory it is possible to quantitatively account for the properties of many correlated solids (Ref. 22). When the dimension is lowered, DMFT becomes less accurate, even though it can account for several properties of two-dimensional systems. For instance, the evolution of optical spectral weight in the cuprates has been successfully described within DMFT (Ref. 23). The situation under investigation is somewhat intermediate between two and three dimensions. We have no reason to think that DMFT will fail, at least as far as the polaron-formation physics is concerned.
[22] G. Kotliar, S. Y. Savrasov, K. Haule, V. S. Oudovenko, O. Parcollet, and C. A. Marianetti, Rev. Mod. Phys. **78**, 865 (2006).
[23] A. Comanac, Luca de Medici, Massimo Capone, and A. J. Millis, Nat. Phys. **4**, 287 (2008); A. A. Toschi, M. Capone, M. Ortolani, P. Calvani, S. Lupi, and C. Castellani, Phys. Rev. Lett. **95**, 097002 (2005).
[24] M. Potthoff and W. Nolting, Phys. Rev. B **59**, 2549 (1999); **60**, 7834 (1999); S. Schwieger, M. Potthoff, and W. Nolting, *ibid.* **67**, 165408 (2003).
[25] A. Liebsch, Phys. Rev. Lett. **90**, 096401 (2003).
[26] R. Matzdorf, Z. Fang, Ismail, J. Zhang, T. Kimura, Y. Tokura, K. Terakura, and E. W. Plummer, Science **289**, 746 (2000).
[27] M. Potthoff and W. Nolting, Phys. Rev. B **52**, 15341 (1995).
[28] R. W. Helmes, T. A. Costi, and A. Rosch, Phys. Rev. Lett. **101**, 066802 (2008).
[29] G. Borghi, M. Fabrizio, and E. Tosatti, Phys. Rev. Lett. **102**, 066806 (2009).
[30] H. Ishida and A. Liebsch, Phys. Rev. B **79**, 045130 (2009).
[31] D. Kalkstein and P. Soven, Surf. Sci. **26**, 85 (1971).
[32] M. Caffarel and W. Krauth, Phys. Rev. Lett. **72**, 1545 (1994).
[33] M. Potthoff and W. Nolting, Z. Phys. B: Condens. Matter **104**, 265 (1997).
[34] M. Capone and S. Ciuchi, Phys. Rev. B **65**, 104409 (2002).